



Deposition of CeO₂/TCP Thin Film on Stainless Steel 316 L by RF sputtering

Hiba A. Abdullah^{a*}, Ahmed M. Al-Ghaban^b, Rana A. Anaee^c

^a University of Technology, Baghdad, Iraq, 10444@uotechnology.edu.iq

^b University of Technology, Baghdad, Iraq, 130127@uotechnology.edu.iq

^c University c of Technology, Baghdad, Iraq, 130033@uotechnology.edu.iq

*Corresponding author.

Submitted: 05/11/2020

Accepted: 05/01/2021

Published: 25/04/2021

KEYWORDS

CeO₂; RF sputtering;
TCP; cerium oxide.

ABSTRACT

RF sputtering method was used for deposition 70wt% CeO₂/TCP thin film on stainless steel 316L surface. The selection of ceria and tricalcium phosphate is according to the fact the importance of these materials in biomedical media. The produced coating was characterized by XRD, FESEM/EDS and AFM analysis, the result revealed that the obtained peaks from XRD refer to the deposited materials. When substitution of Ce was done, distorting of the lattice structure can occur suggesting certain incorporation of the cerium oxide within TCP lattice. Also, from SEM investigation uniformly homogeneous surface as a layer of (CeO₂ + CaO) and TCP as sharp plate-like crystals. EDS analysis of coating confirms the presence of Ce, Ca, O and P elements, thickness was determined at 130.7 nm. The soaking in Simulation body fluid indicated the formation of layers like hydroxyapatite, which investigated by XRD and FESEM/EDS methods.

How to cite this article: H. A. Abdullah, A.M. Al-Ghaban, and R. A. Anaee, "Deposition of Thin Film of CeO₂/TCP on Stainless Steel 316 L by RF sputtering," Engineering and Technology Journal, Vol. 39, Part A, No. 04, pp. 625-631, 2021.

DOI: <https://doi.org/10.30684/etj.2021.168140>

This is an open access article under the CC BY 4.0 license <http://creativecommons.org/licenses/by/4.0>

1. INTRODUCTION

Sputtering techniques have been widely used as a coating method during the last decade, as the DC and RF sputtering method in their two design; balanced and unbalanced magnetron in industrial applications such as thin films for decoration purposes, hard films to reduce wear and friction and increase corrosion resistance, and thin films used as a protective optical system, in addition to applications in the electronic industry. In addition to the effect of the deposition parameters (substrate temperature, working pressure, density power utilized to the target), the application in the research field involves the interaction between the charged ions and the surface of the target material, the adherence between the substrate and the deposited particle and chemical reactions above the substrate. The surface of titanium substrates was modified as mentioned in many studies by using a

TCP coating by using a radio frequency magnetron (RF) sputtering as coating method and with different powers ranging from 75 to 150 W [1], for hard-tissue implant applications onto Ti-6Al-4V substrates using RF magnetron sputtering [2, 3], and deposition of CaP by RF magnetron sputtering onto 316L SS [4-6]. Also, studies that included the deposition of CaP coating, whose thickness ranges between 0.1 to 2.7 μm on the implant that are used as biomaterials, and the results of these coatings were homogeneous, uniform and dense without defects visible on the deposited layer [7]. Rare earth metals have advantages, especially (Ce) in bio application due to low toxicity to improve the corrosion resistance, hot workability and mechanical properties of stainless steels. There are many studies related to coating by CeO_2 [8-16]. Therefore, we suggested depositing cerium oxide/TCP coating on SS 316L to investigate the role of the suggested produced coating for bio applications by the RF sputtering method due to the advantages of this method.

2. EXPERIMENTAL PART

I. Sample Preparation

Stainless steel 316 L specimens were used as a substrate to apply the coating of CeO_2 /TCP, the chemical composition of these specimens is (wt%: 0.022 C, 0.407 Si, 1.43 Mn, 0.031 P, 0.004 S, 16.98 Cr, 2.00 Mo, 11.73 Ni, 0.234 Cu and Fe remains) obtained by Bruker advanced X-ray solution D8-advance. The specimens were cut a square shape with a dimension of 2×2 cm and then grained with SiC paper (600, 800, 1000, and 1200 grit size) after that they were polished with alumina paste. The substrates were ultrasonically cleaned in a diluted acetone bath for 25 min, then distilled water is used as a rinse to ensure the surface of the substrate is free of acetone alcohol residue and other impurities.

II. Coating Process

Cerium substituted TCP thin film was deposited on SS 316L substrate by RF magnetron sputtering at 150 °C (Model No. CRC 600, Serial No. MST-CRC-102510-ND2-MS as shown in Figure 1). 70 wt% CeO_2 /30 wt% TCP target was prepared using commercially available CeO_2 powder (E. Merck, Darmstadt, 99.99 %) and TCP (HIMEDIA, 99.99 %). A pellet of 50 mm diameter and 5 mm thickness was prepared from compacting the powders in a stainless-steel pelletizer under 5 tones as pressure by a hydraulic press, and then this pellet was charged to a furnace for sintering at 1100 °C for 3 hrs.

All experiments were carried out under Ar gas to generate plasma in the sputtering chamber with pressure (3×10^{-4} mbar), gas flow rate (5 sccm), deposition time (30 min), RF power (150W) and temperature of the substrate (150 °C).



Figure 1: RF Magnetron sputtering system.

III. Characterization Methods

The characterization of thin films was done by XRD with CuK α radiation ($k = 1.5418 \text{ \AA}$), FESEM/EDS analysis (FEI QUANTA 250, Czech Republic) and AFM (SPM 600, Agilent Technologies).

3. RESULTS AND DISCUSSION

I. Characterization

Figure 2 shows the XRD analysis of SS 316 L substrate, this analysis indicates the diffraction peaks related to the crystalline phase of stainless steel 316 L according to (JCPDS card No. 33-0397). The incorporation was done by adding 70wt% cerium oxide to TCP. The XRD analysis of the CeO₂/TCP coated SS 316 L sample indicates clearly the 2θ value at ≈38.2 which is attributed to calcium oxide according to (JCPDS card No. 09-0169). In addition, cerium oxide leads to appear new intensity at 2θ ≈ 28.17, this is an indication of the presence of CeO₂ according to (JCPDS card No. 43-1002).

In this XRD pattern, it can be noticed significantly the overlapping of the obtained peaks. When substitution of Ce was done, distorting of the lattice structure can occur suggesting certain incorporation of the cerium oxide within TCP lattice. As a result of the large incorporation of cerium oxide into the appetite network [17, 18], a slight shift was observed; resulting in peaks recorded at a lower degree, the reason for this behavior is the effect of substitutions that change the crystal structure [19].

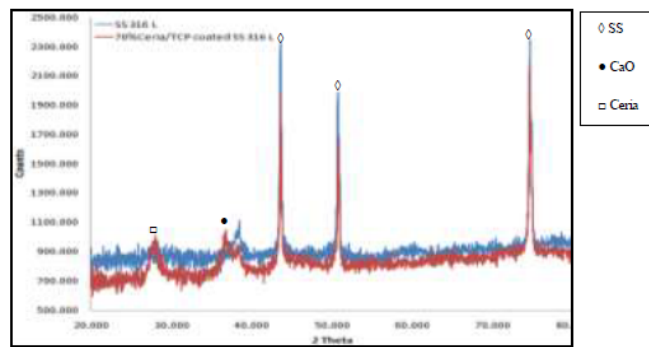


Figure 2: XRD of uncoated and coated SS 316L.

Figure 3 indicates the FESEM/EDS of the polished SS 316L surface with little atmospheric corrosion. Also, this image shows a characteristic inclusion observed on the surface. EDS analysis shows the main elements in SS 316L (Fe, Cr and Ni) in addition to oxygen obtained from the iron oxide layer due to the little atmospheric corrosion. The addition of CeO₂ (70 wt%) to TCP led to give more uniformly homogeneous surface (Figure 4) as a layer of (CeO₂ + CaO) and TCP as sharp plate like crystals. EDS analysis of coating confirms the presence of Ce, Ca, O and P elements.



Figure 3: FESEM/EDS of SS 316L substrate

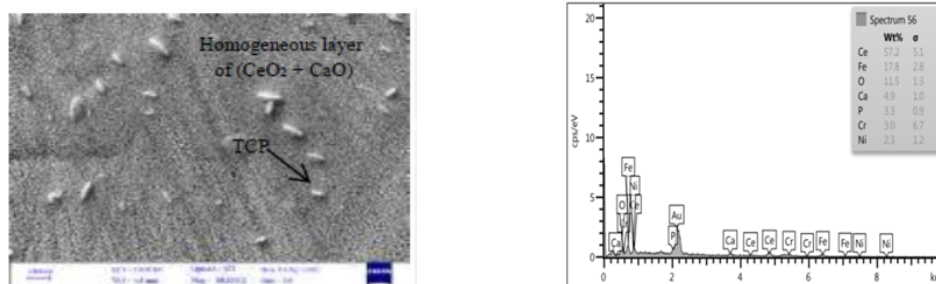


Figure 4: FESEM/EDS of 70% CeO₂/TCP coated SS 316 L.

The cross-section of the coated layer was investigated by FESEM to know the thickness as shown in Figure 5 which was 130.7 nm.

EDS mapping of SS 316L is shown in Figure 6, while the coating is shown in Figure 7 revealing the elemental distribution of the metal ions. For SS 316L surface, it is clear the distribution of the main elements in the substrate (Fe, Ni and Cr). For the CeO₂/TCP coated specimen, can be seen the presence of calcium (Ca), oxygen (O), cerium (Ce) and phosphor (P).

AFM images give an indication of the topography of coated surfaces. 2D and 3D images for SS 316L surface as shown in Figure 8 indicate a smooth surface with very little roughness (1.4 nm) due to little atmospheric corrosion and with a low summit (7.42). A rougher surface (1.69 nm) and higher summit (14.27 nm) can be observed for 70%CeO₂/TCP coated surface (Figure 9).

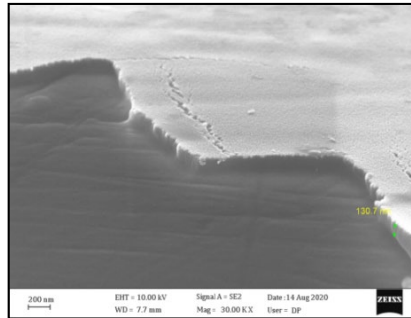


Figure 5: Cross-section of the coated specimen

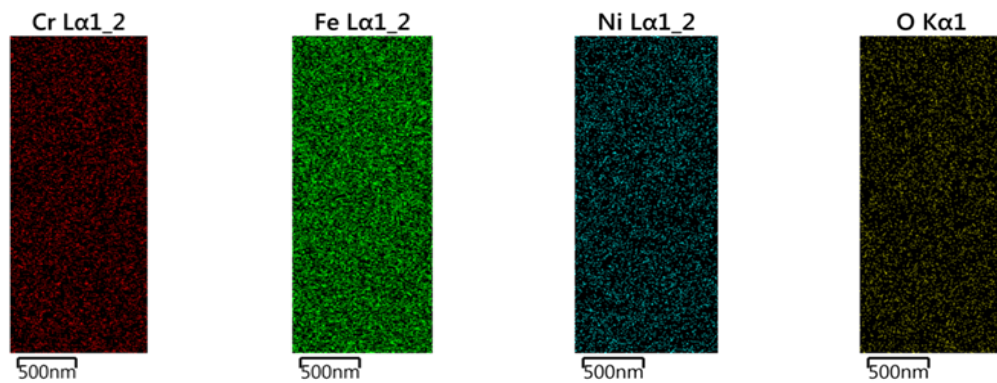


Figure 6: EDS mapping for SS 316L.

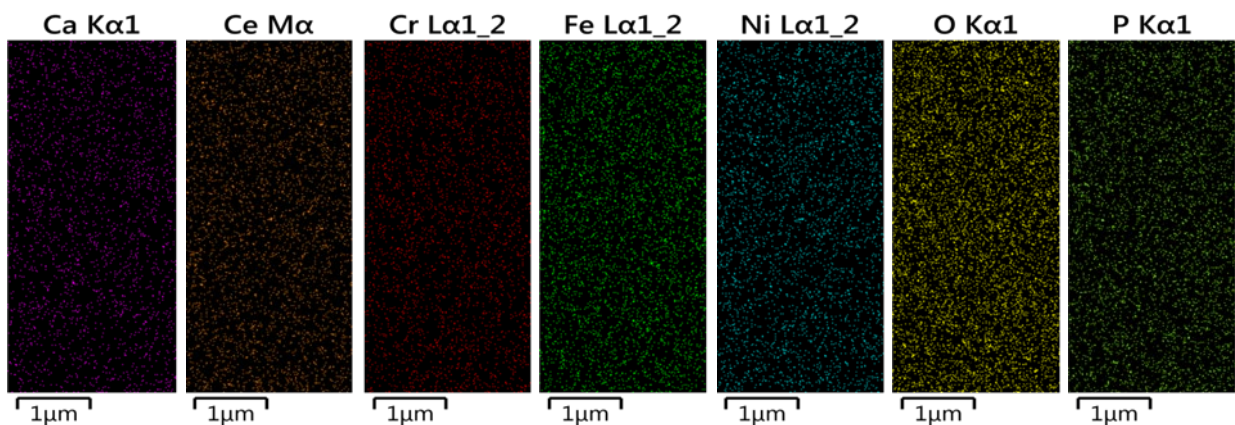


Figure 7: EDS mapping of 70% CeO₂/TCP coated SS 316 L

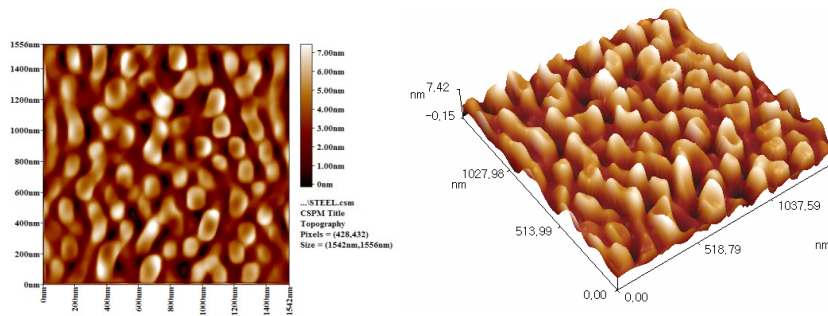


Figure 8: AFM images SS 316 L.

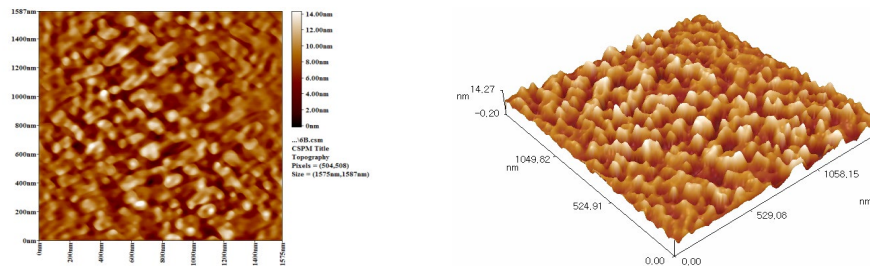


Figure 9: AFM images of 70% CeO₂/TCP coated SS 316 L.

II. Formation of Hydroxyapatite Layer

The immersion in simulated body fluid (SBF) for 14 days suggests the formation of layer like hydroxyapatite. The formed layer was examined by XRD and FESEM/EDS techniques. The XRD analysis is shown in Figure 10 which indicates the peaks of stainless steel and considered the peaks at intensity equal 100% for Ca₃(PO₄)₂ at 2θ of 34.128 and for CeO₂ at 2θ 28.5 and for Ca₃Ce (PO₄)₃ at 2θ of 28.354. In addition to observing the peaks of hydroxyapatite at 2θ of 32.054 (100), 25.879 (40), 46.788 (20) and 49.496 (20) according to (JCPDS card No. 01-1008). FESEM/EDS analysis was done for some specimens that showed the presence of a new phase.

Figure 11 indicates FESEM/EDS images for a coated specimen which shows the growth of hydroxyapatite on the material after it was soaked in SBF for 14 days [20], also it can be seen that hydroxyapatite crystals form spherical shapes (cauliflower morphology) with particle size ranged from 57.69 to 83.74 nm. The EDS analysis confirms the incorporation of cerium within the formed hydroxyapatite layer on the substrate.

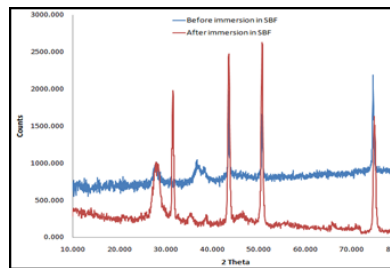


Figure 10: XRD of coated specimens before and after immersion in SBF

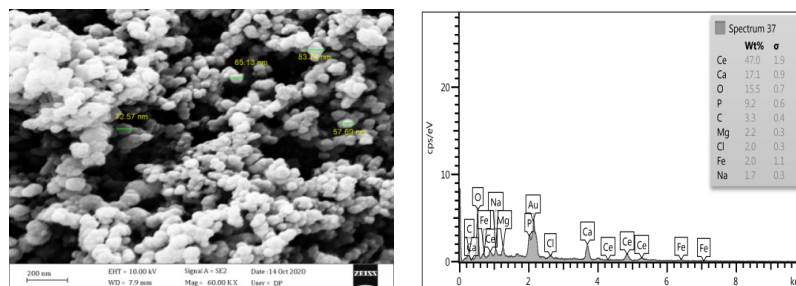


Figure 11: FESEM/EDS of coated specimens after immersion in SBF.

III. Biological Properties

Figure 12 shows the biocompatibility test for Ce substitution TCP coating. This figure indicates the good biocompatibility of Ce/TCP coating after 24, 48 and 72 hrs of incubation, the material's surface was completely covered by cell layer, and the coverage increases with increasing the incubation time.

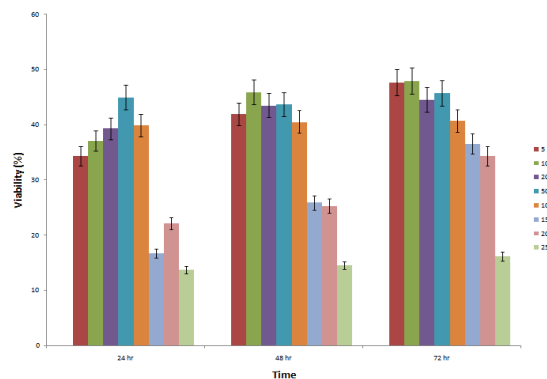


Figure 12: Biocompatibility Ce/TCP deposited on SS 316L.

The antibacterial result is shown in Figure 13, which reveals that the antibacterial responsibility for Ce/TCP coating is more than for uncoated SS 316L, the reason may be the incorporation of mineral cerium which plays a vital role in enhancing the antibacterial activity.

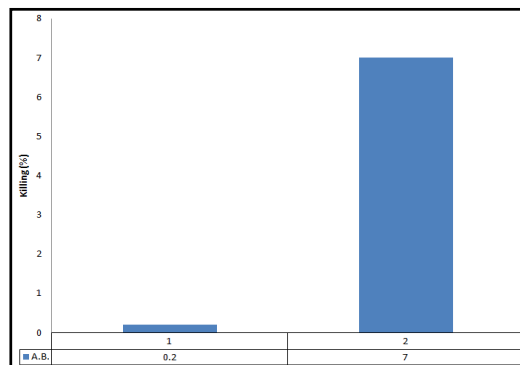


Figure 13: Antibacterial test for uncoated and coated SS 316L

4. CONCLUSION

The doping by ceria for tricalcium phosphate as a thin film was successful by RF sputtering technique through preparing target of 70 wt% CeO₂ – 30 wt% β-TCP by applying 150W and the substrate was kept at 150 °C. The characterization techniques confirmed this doping, in addition, to improve the incorporation of the implant with tissue through the formation of hydroxyapatite layer after immersion in SBF for 14 days and then investigate the formed layer by XRD and FESEM/EDS methods.

References

- [1] T. Narushima , K. Ueda , T. Goto , H. Masumoto, T. Katsube, H. Kawamura, Ch. Ouchi , Y. Iguchi, Preparation of calcium phosphate films by radiofrequency magnetron sputtering, Mater. Trans., 46 (2005) 2246-2252. <https://doi.org/10.2320/matertrans.46.2246>
- [2] A.R. Boyd, B. J. Meenan, N. S. Leyland, Surface characterisation of the evolving nature of radio frequency (RF) magnetron sputter deposited calcium phosphate thin films after exposure to physiological solution, Surf. Coat. Technol., 200 (2006) 6002–6013. <https://doi.org/10.1016/j.surfcoat.2005.09.032>
- [3] D. K. Pattanayak, R. Dash, R. C. Prasad, B. T. Rao, T. R. R. Mohan, Synthesis and sintered properties evaluation of calcium phosphate ceramics, Mater. Sci. Eng. C., 27 (2007) 684–690. <https://doi.org/10.1016/j.msec.2006.06.021>

- [4] J. Toque, M. Hamdiy, A. Ide-Ektessabiz, I. Sopyanx, Effect of the processing parameters on the integrity of calcium phosphate coatings produced by RF-magnetron sputtering, *Int. J. Mod. Phys. A.*, 23 (2009) 5811-5818. <https://doi.org/10.1142/S021797920905479x>
- [5] J. A. Toquea, M. K. Herliansyah, M. Hamdib, A. Ide-Ektessabic, I. Sopyan, Adhesion failure behavior of sputtered calcium phosphate thin film coatings evaluated using microscratch testing, *J. Mech. Behav. Biomed. Mater.*, 3 (2010) 324-330. <https://doi.org/10.1016/j.jmbbm.2010.01.002>
- [6] K. Y. Hung, H. C. La, H. P. Feng, Characteristics of RF-sputtered thin films of calcium phosphate on titanium dental implants, *Coat.*, 7 (2017) 126. <https://doi.org/10.3390/coatings7080126>
- [7] V. F. Pichugin, S. I. Tverdokhlebov, R. A. Surmenev, E. V. Shesterikov, M. A. Riabtseva, A. A. Kozelskaya, I. A. Shulepov, Surface morphology and properties of calcium phosphate thin films formed by plasma of RF-magnetron discharge, *Phys. Basis. Radiation – Related Techno.*, 49(2006)320- 323.
- [8] H. Jing, X. Wu, Y. Liu, M. Lu, K. Yang, Z. Yao, W. Ke, Antibacterial property of Ce-bearing stainless steels, *J. Mater. Sci.*, 42 (2007) 5118–5122. <https://doi.org/10.1007/s10853-006-0603-9>
- [9] S. M. Hirst, A. S. Karakoti, R. D. Tyler, N. Sriranganathan, S. Seal, Ch. M. Reilly, Anti-inflammatory properties of cerium oxide nanoparticles, *Small.*, 5 (2009) 2848–2856. <https://doi.org/10.1002/sml.200901048>
- [10] O. Lavigne, C. A. Dumont, B. Normand, P. Delichère, A. Descamps, Cerium insertion in 316L passive film: Effect on conductivity and corrosion resistance performances of metallic bipolar plates for PEM fuel cell application, *Surf. Coat. Technol.*, 205 (2010) 1870–1877. <https://doi.org/10.1016/j.surfcoat.2010.08.051>
- [11] I. Celardo, J. Z. Pedersen, E. Traversab, L. Ghibelli, Pharmacological potential of cerium oxide nanoparticles, *Nanoscale. Adv.*, 3 (2011) 1411-1420. <https://doi.org/10.1039/C0NR00875C>
- [12] Y. Junping, L. Wei, Sh. Keya, Study of Ce-modified antibacterial 316L stainless steel, *Res. Develop.*, 9 (2012) 307-312.
- [13] E. Stoyanova, D. Stoychev, Corrosion behavior of stainless steels modified by cerium oxides layers, Publisher InTech, 1st edition, Bulgaria, [Online], Available. (2012) 239-241.
- [14] M. Dubau, J. Lavková, I. Khalakhan, S. Haviar, V. Potin, V. Matolín, I. Matolínová, Preparation of magnetron sputtered thin cerium oxide films with a large surface on silicon substrates using carbonaceous interlayers, *ACS Appl. Mater. Interfaces.*, 6 (2014) 1213–1218. <https://doi.org/10.1021/am4049546>
- [15] G. Ciofani, G. G. Genchi, I. Liakos, V. Cappello, M. Gemmi, A. Athanassiou, B. Mazzolai, V. Mattoli, Effects of cerium oxide nanoparticles on pc12 neuronal-like cells: proliferation, differentiation, and dopamine secretion, *Pharmaceutical Research.* 30(2013)2133-2145. <https://doi.org/10.1007/s11095-013-1071-y>
- [16] D. Rajeswari, D. Gopi, S. Ramya, L. Kavitha, Investigation of anticorrosive, antibacterial and in-vitro biological properties of sulphonated poly (etheretherketone)/strontium, cerium co-substituted hydroxyapatite composite coating developed on surface treated surgical grade stainless steel for orthopedic applications, *RSC Adv.*, 4 (2014) 61525-61536. <https://doi.org/10.1039/C4RA12207K>
- [17] X. Yin, M. J. Stott, A. Rubio, A- and b-tricalcium phosphate: A density functional study, *Phys. Rev., B.* 68 (2003) 205205. <https://doi.org/10.1103/PhysRevB.68.205205>
- [18] X. Wang, Q. Zhang, S. Mao, W. Cheng, A theoretical study on the electronic structure and floatability of rare earth elements (La, Ce, Nd and Y) bearing fluorapatite, *Minerals*, 9 (2019) 500. <https://doi.org/10.3390/min9080500>
- [19] A. Matraszek, I. Szczygiel, Phase relationships in the tricalcium phosphate—cerium phosphate system. thermal behavior of phases presents in the system, *J. Am. Ceram. Soc.*, 95 (2012) 3651–3656. <https://doi.org/10.1111/j.1551-2916.2012.05384.x>
- [20] L. A. Adams, E. R. Essien, R. O. Shaibu, A. Oki, Sol-gel synthesis of SiO₂-CaO-Na₂O-P₂O₅ bioactive glass ceramic from sodium metasilicate, *J. Glass. Ceram.*, 3 (2013) 11-15. <https://doi.org/10.4236/njgc.2013.31003>